Turbulent and non-turbulent optical angle-of-arrival and irradiance fluctuations in the stably stratified atmosphere

Andreas Muschinski

NorthWest Research Associates (NWRA)
Boulder, Colorado

Program Review 2014: Remote Sensing and Imaging Physics
Kirtland Air Force Base, New Mexico
18/19 November 2014

Introduction

- Motivation: why a propagation testbed?
- Equipment and experimental setup
- Retrieval of temporal dT/dz fluctuations
- Retrieval of optical turbulence intensity (C_n^2, C_T^2)
- Retrieval of transverse wind velocities
- Summary and a conclusion

Motivation:
Why a propagation testbed?

- Need to test hypotheses and approximations (e.g., homogeneity, isotropy and stationarity of turbulence; Taylor hypothesis; Markov approximation; geometrical-optics approximation; negligibility of fluctuating aerosol concentrations)

- Need to compare optical observations/retrievals with accurate, precise, fast-response, simultaneous, in-situ observations along the propagation path.

Equipment and experimental setup

Equipment:

- Telescopes
- CCD cameras
- Ultrasonic anemometers/thermometers (“sonics”)
- Test-light arrays

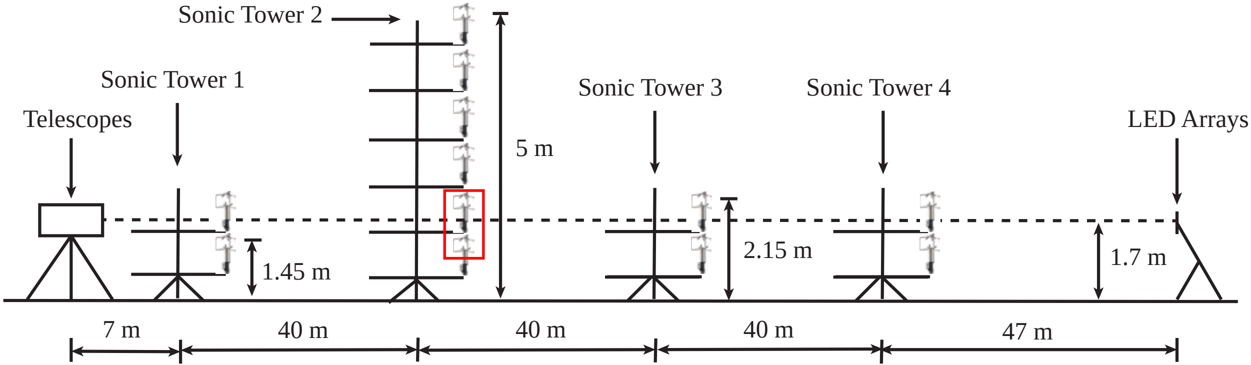

Figure 1: *Experimental setup of several optical propagation experiments conducted in August, 2012 at the Boulder Atmospheric Observatory near Erie, CO. Only data from the two sonics marked by the red box have been used for the present study.*

Four “sonics”
mounted on a portable tower,
crossed-beam experiment,
BAO, April 11, 2014

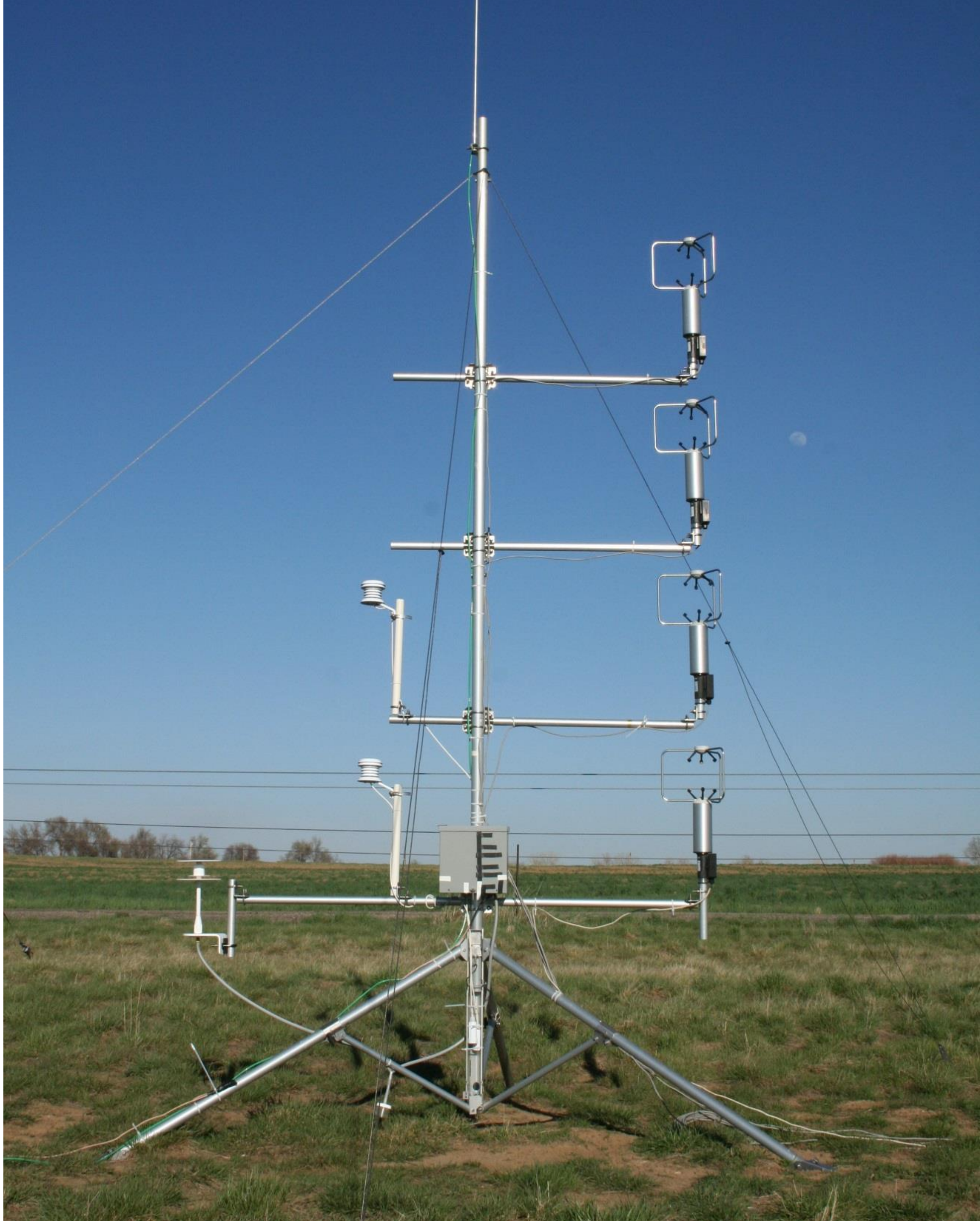

Test-light array (TLA),
crossed-beam experiment,
BAO, April 11, 2014

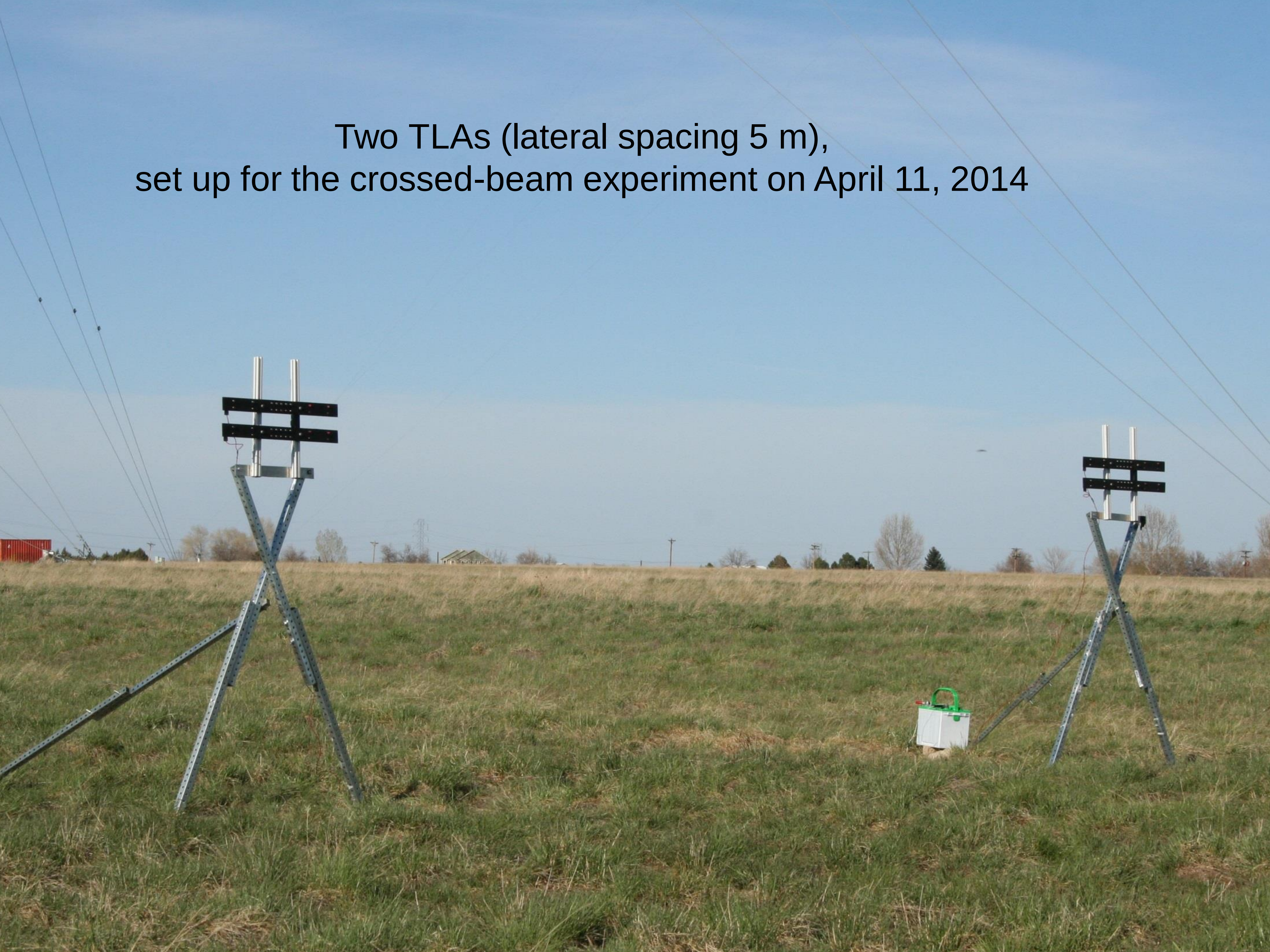

Two TLAs (lateral spacing 5 m),
set up for the crossed-beam experiment on April 11, 2014

Two telescopes (14 inch aperture),
set up for the crossed-beam experiment on April 11, 2014

Telescopes

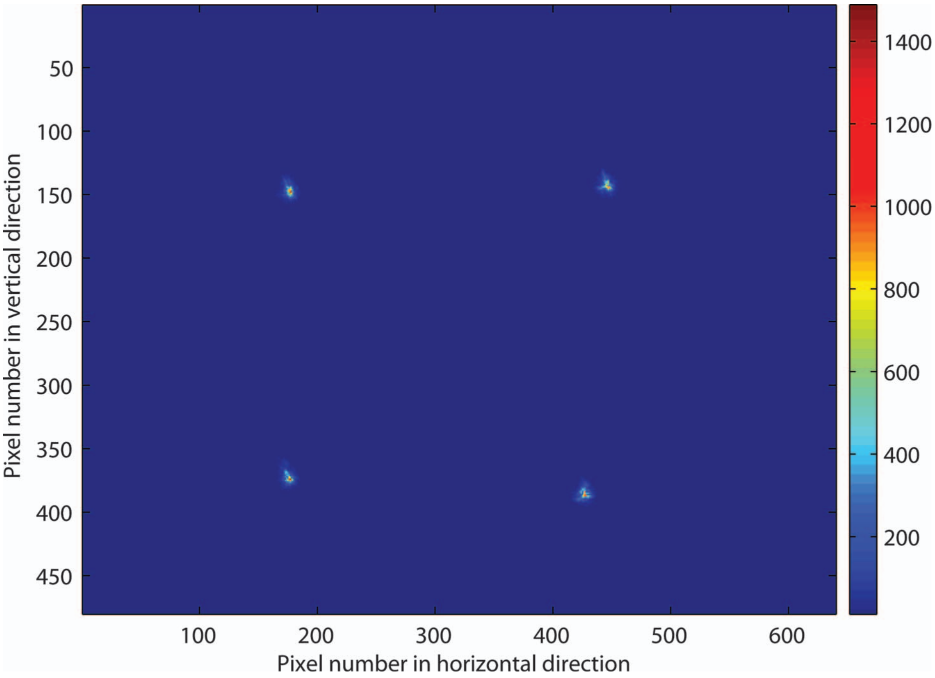

Fig. 3. Image of four lights measured at 21:00:10 LT, September 27, 2006.

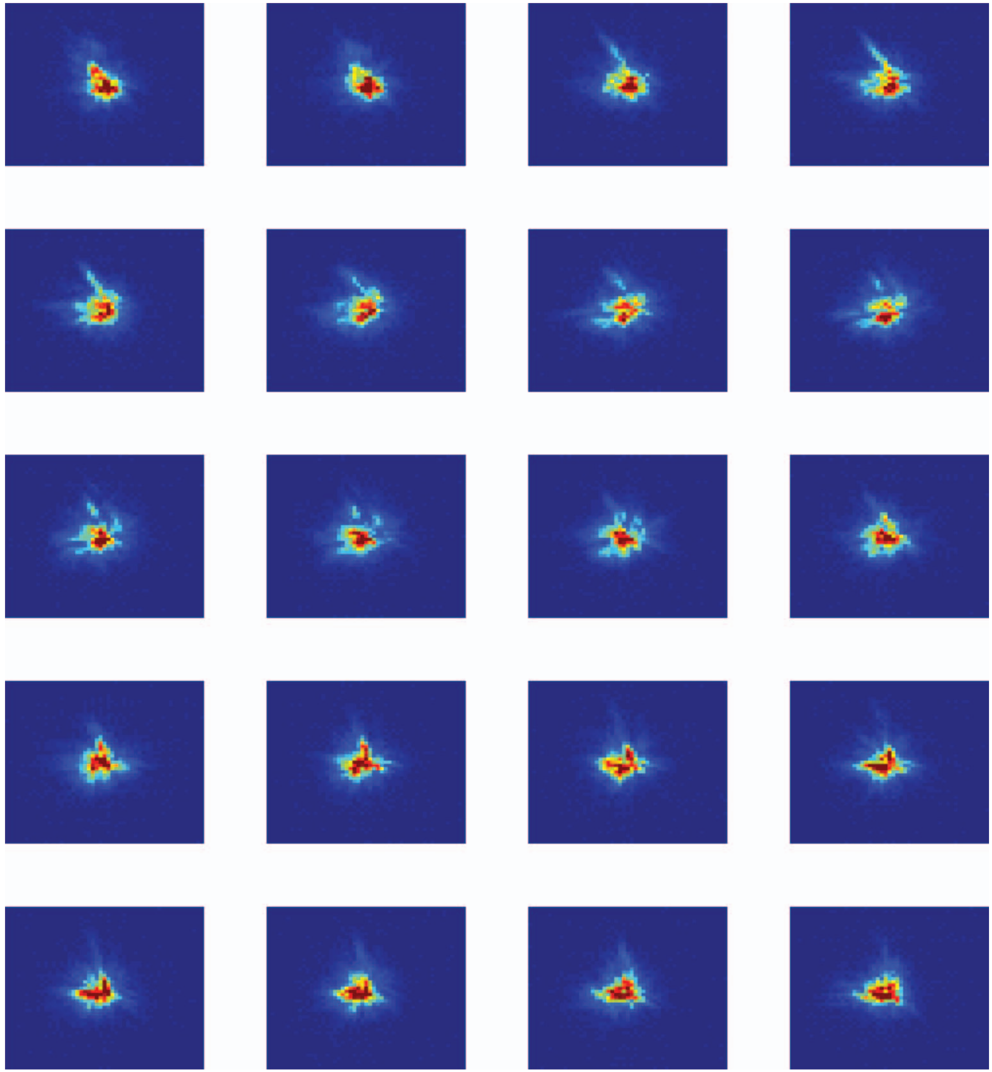

Fig. 4. Sequence of subimages (51 × 51 pixels) of the bottom left-hand light, measured at 21:00:10.9–21:00:11.6 LT, September 27, 2006. The first row, first column is the first image, the first row, fourth column is the fourth image.

Retrieval of temporal dT/dz fluctuations

Basic theory of refraction

Optical **refractive index** of air:

$$n = 1 + a\frac{p}{T}, \tag{1}$$

where a = constant = $7.9 \cdot 10^{-7}\mathrm{K\,Pa^{-1}}$, p = air pressure, T = air temperature.

Vertical component of the **angle-of-arrival** if source and telescope are at the same height (from eikonal equation):

$$\alpha = -\frac{\Delta\alpha}{2} = \frac{1}{2}\int_0^L \frac{\partial n(x,z)}{\partial z}dx, \tag{2}$$

where $\Delta\alpha$ = total refraction, x = path coordinate, z = vertical coordinate,
L = path length.

Hydrostatic equation and ideal **gas equation**:

$$\frac{\partial p}{\partial z} = -\rho g = -\frac{p}{R_a T}g, \tag{3}$$

where ρ = air density, g = acceleration due to gravity, $R_a = 287\ \mathrm{J\,kg^{-1}\,K^{-1}}$ = gas constant for (dry) air.

Basic theory of refraction (cont'd)

Insert (1) and (3) into (2) to get the **AOA in terms of the path average of the vertical temperature gradient** $\gamma = \frac{\partial T}{\partial z}$:

$$\alpha = \frac{aL}{2} \frac{p}{T^2} \left(\frac{g}{R_a} + \gamma \right). \tag{4}$$

Sensitivity of AOA with respect to γ:

$$s = \frac{\partial \alpha}{\partial \gamma} = \frac{aL}{2} \frac{p}{T^2}. \tag{5}$$

In our case (night of 14/15 August, 2012): $p = 839$ hPa, $T = 288$ K and $L = 174$ m, such that

$$s = 73 \; \frac{\mu\mathrm{rad}}{\mathrm{K\,m^{-1}}} = \frac{1\,\mu\mathrm{rad}}{0.014\,\frac{\mathrm{K}}{\mathrm{m}}}. \tag{6}$$

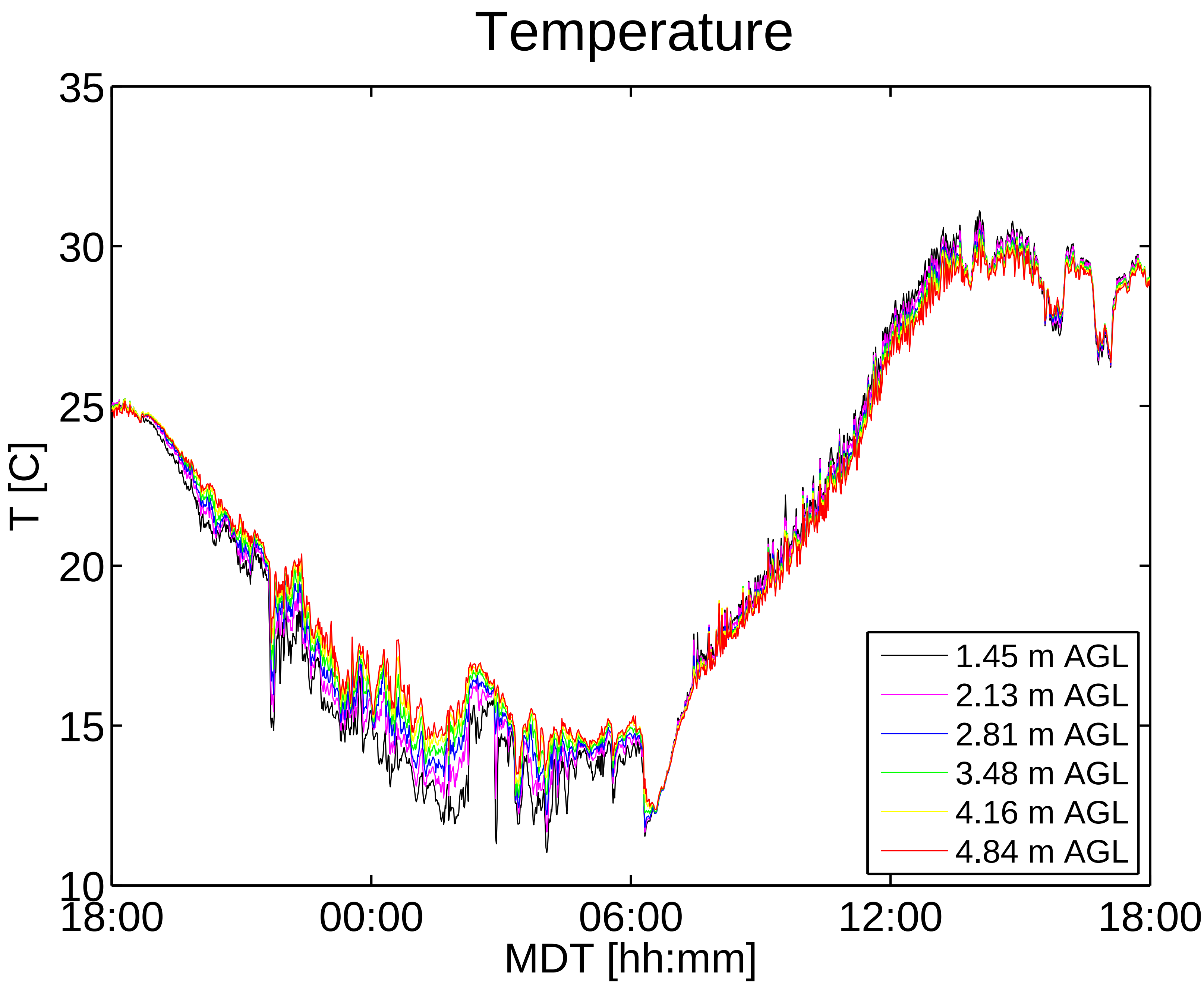

Temperature
35
30
25
20
15
10
T [C]
18:00
00:00
06:00
12:00
18:00
MDT [hh:mm]
1.45 m AGL
2.13 m AGL
2.81 m AGL
3.48 m AGL
4.16 m AGL
4.84 m AGL

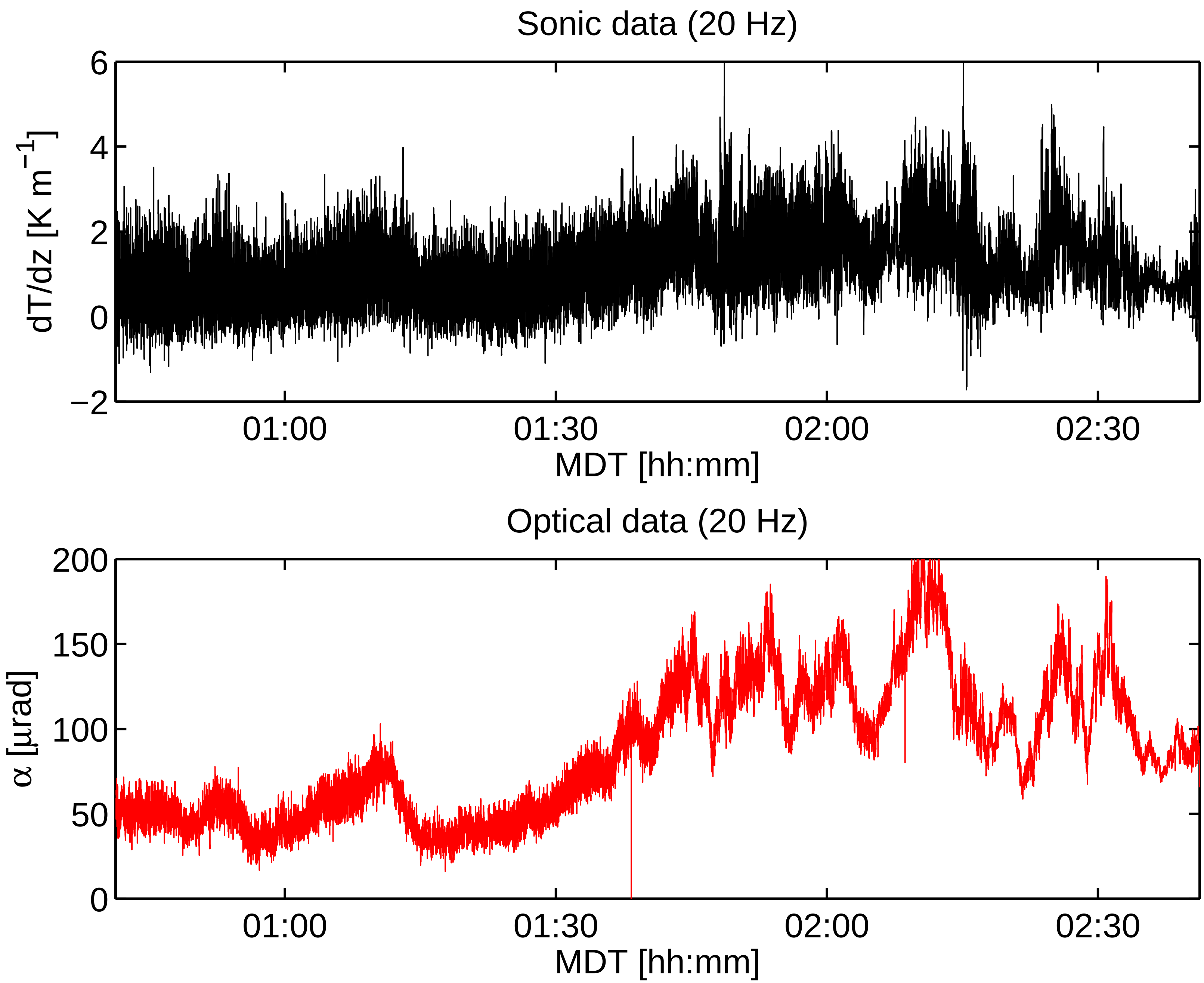
Sonic data (20 Hz)
dT/dz [K m^-1]
6
4
2
0
−2
01:00
01:30
02:00
02:30
MDT [hh:mm]
Optical data (20 Hz)
α [μrad]
200
150
100
50
0
01:00
01:30
02:00
02:30
MDT [hh:mm]

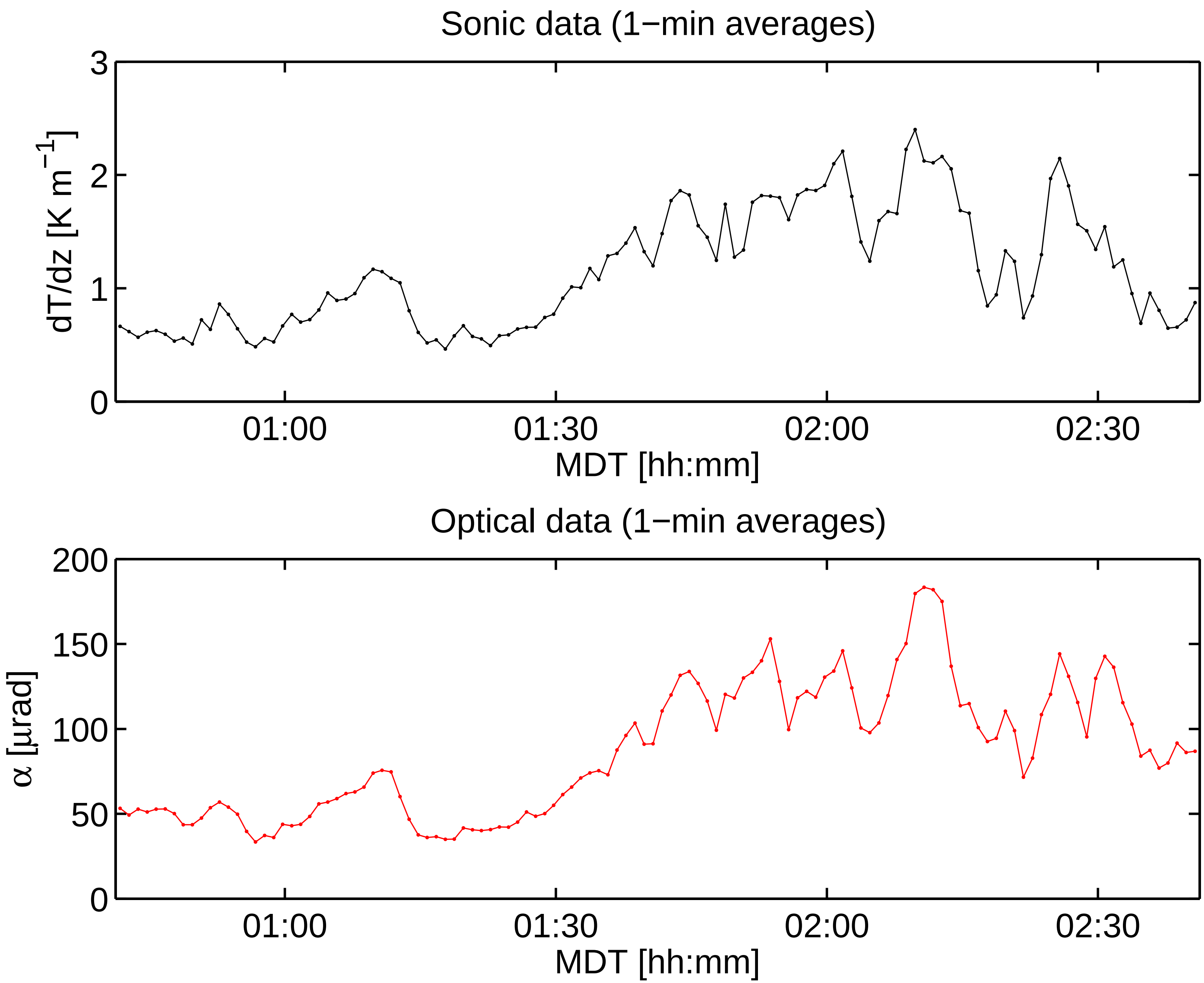
Sonic data (1−min averages)
dT/dz [K m^{-1}]
0
1
2
3
01:00
01:30
02:00
02:30
MDT [hh:mm]
Optical data (1−min averages)
α [μrad]
0
50
100
150
200
01:00
01:30
02:00
02:30
MDT [hh:mm]

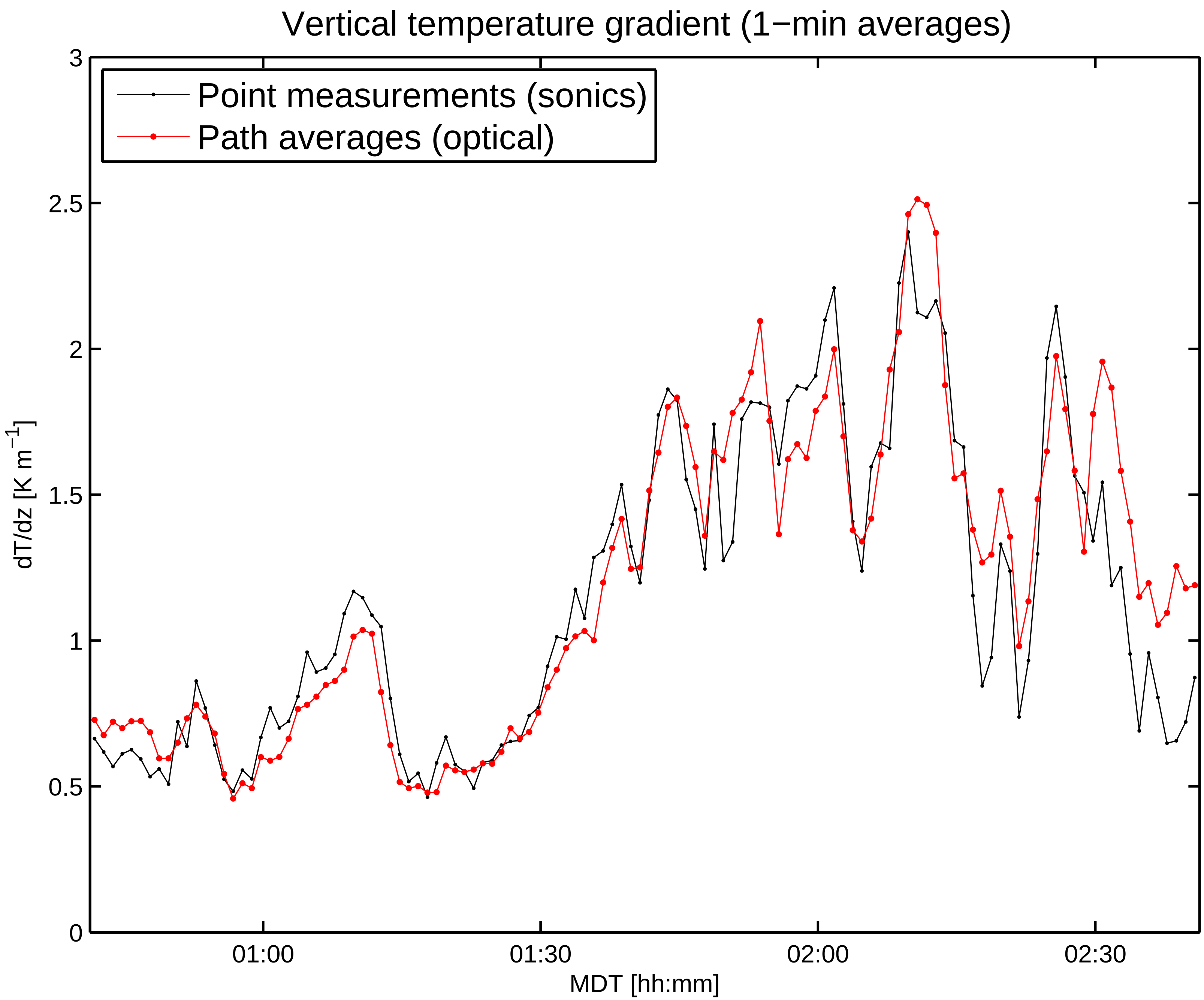

Vertical temperature gradient (1−min averages)
Point measurements (sonics)
Path averages (optical)
dT/dz [K m^{-1}]
MDT [hh:mm]
3
2.5
2
1.5
1
0.5
0
01:00
01:30
02:00
02:30

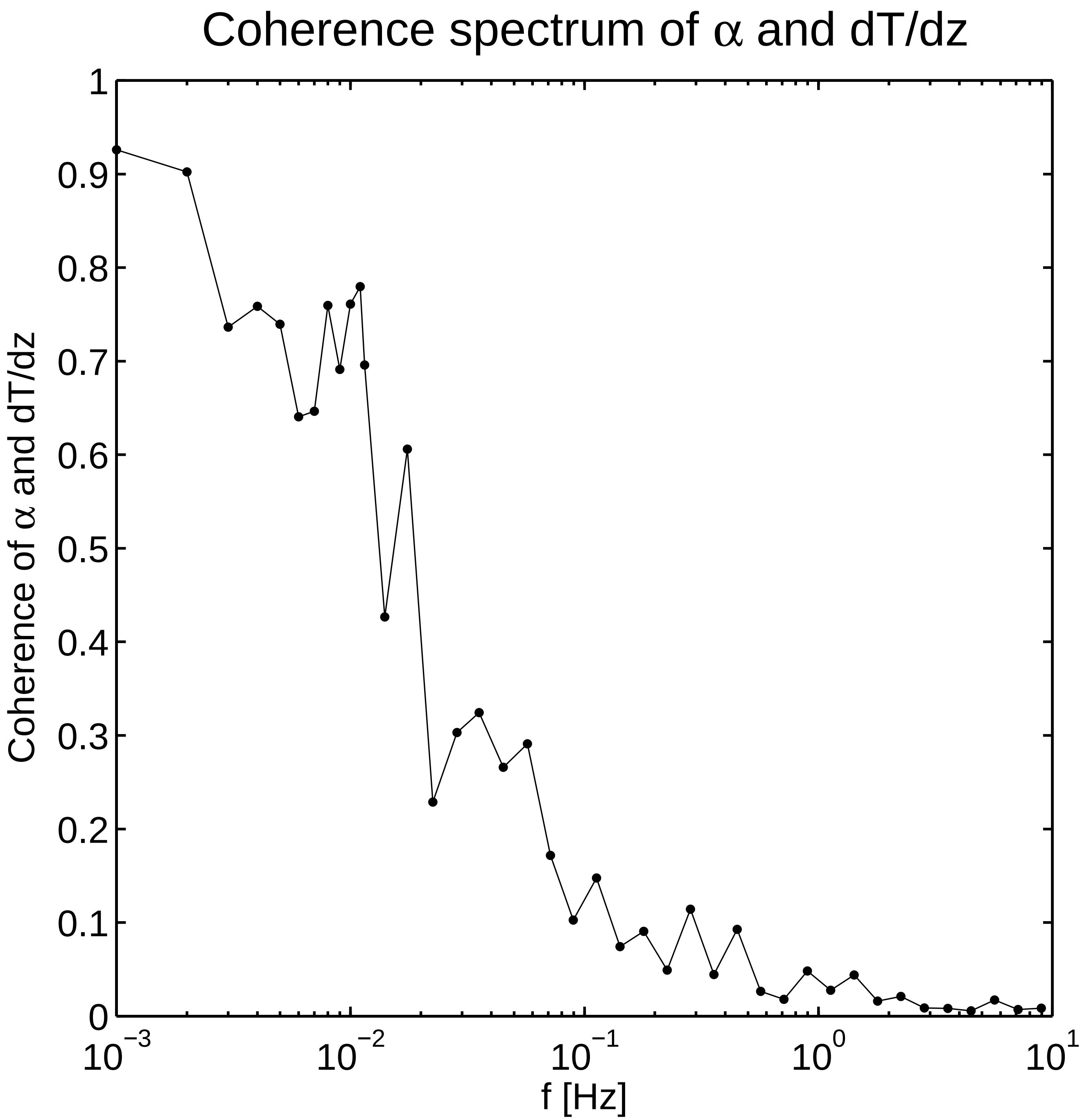

Coherence spectrum of α and dT/dz
Coherence of α and dT/dz
f [Hz]
0
0.1
0.2
0.3
0.4
0.5
0.6
0.7
0.8
0.9
1
10^{-3}
10^{-2}
10^{-1}
10^{0}
10^{1}

Retrieval of optical turbulence intensity (C_n^2, C_T^2)

Theory: C_n^2 and C_T^2

Structure function of a turbulent refractive-index field:

$$D_n(\mathbf{x}, \mathbf{r}) = \langle [n(\mathbf{x} + \mathbf{r}) - n(\mathbf{x})]^2 \rangle, \tag{1}$$

where $\mathbf{x}$ = location and $\mathbf{r}$ = spatial separation

Homogeneous turbulence: $D_n(\mathbf{x}, \mathbf{r})$ is independent of $\mathbf{x}$.
Isotropic turbulence: $D_n(\mathbf{x}, \mathbf{r})$ is independent of $\mathbf{r}$.
Homogeneous and isotropic turbulence: $D_n(\mathbf{x}, \mathbf{r})$ depends only on $r = |\mathbf{r}|$.

Homogeneous and isotropic turbulence in the **inertial subrange** (Obukhov 1949):

$$D_n(r) = C_n^2 r^{2/3}, \tag{2}$$

where C_n^2 is the refractive-index structure parameter. For dry air, where

$$n = 1 + a\frac{p}{T}, \tag{3}$$

we have

$$D_T(\mathbf{x}, \mathbf{r}) = \langle [T(\mathbf{x} + \mathbf{r}) - T(\mathbf{x})]^2 \rangle = a^2 \frac{p^2}{T^4} \langle [n(\mathbf{x} + \mathbf{r}) - n(\mathbf{x})]^2 \rangle, \tag{4}$$

such that for inertial-range turbulence the temperature structure parameter is

$$C_T^2 = a^2 \frac{p^2}{T^4} C_n^2. \tag{5}$$

For **optical turbulence** in the inertial subrange, the variance of the vertical AOA fluctuations, σ_α^2, is equal to the variance of the horizontal AOA fluctuations, σ_β^2:

$$\sigma_\alpha^2 = \sigma_\beta^2. \tag{6}$$

By means of geometrical optics, we obtain for a spherical wave propagating through inertial-range turbulence and received with a circular aperture:

$$\sigma_\alpha^2 = \sigma_\beta^2 = 1.064\, L D^{-1/3} C_n^2, \tag{7}$$

where L = propagation path length and D = telescope's aperture diameter.

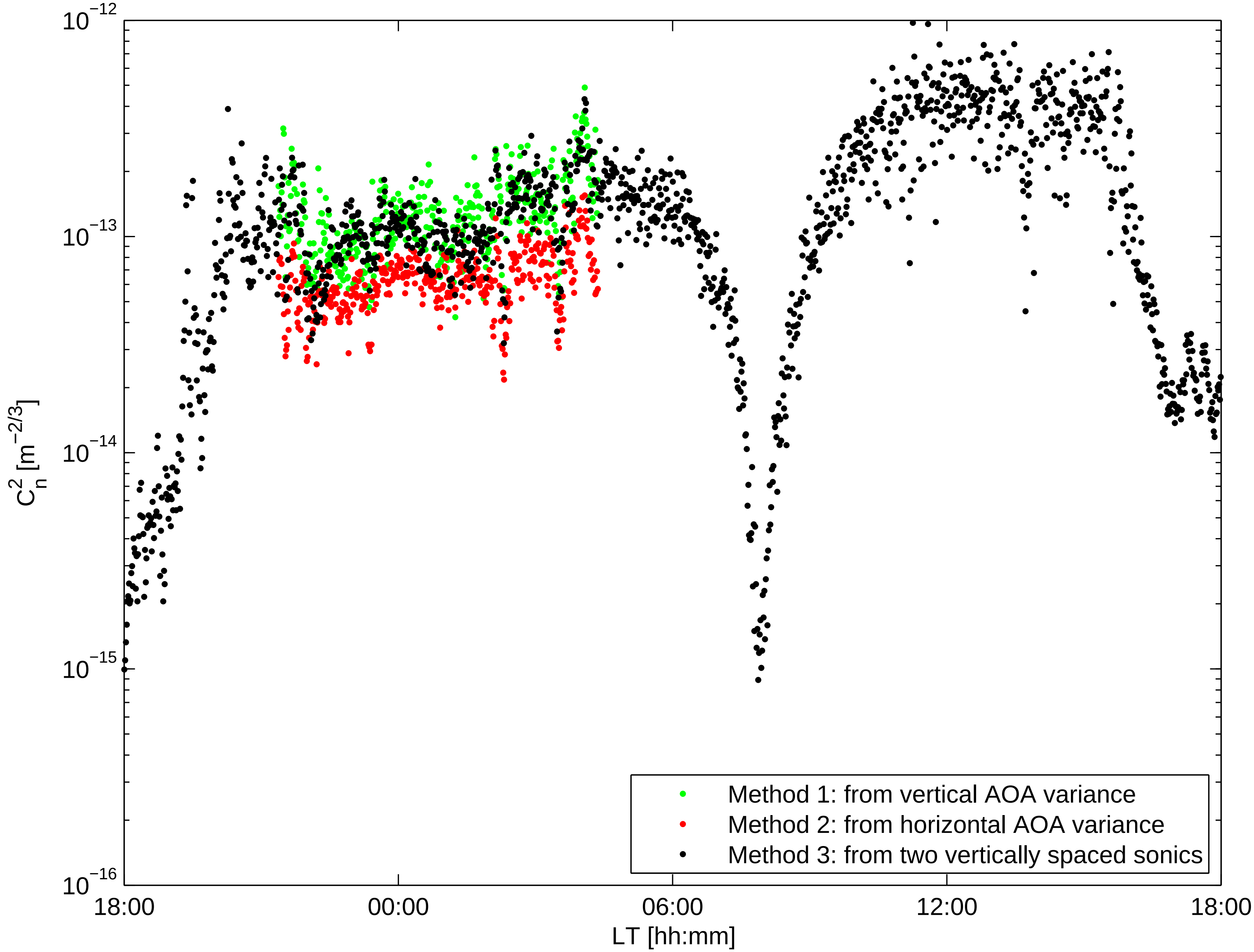

10^{-12}
10^{-13}
10^{-14}
10^{-15}
10^{-16}
C_n^2 [$m^{-2/3}$]
18:00
00:00
06:00
12:00
18:00
LT [hh:mm]
Method 1: from vertical AOA variance
Method 2: from horizontal AOA variance
Method 3: from two vertically spaced sonics

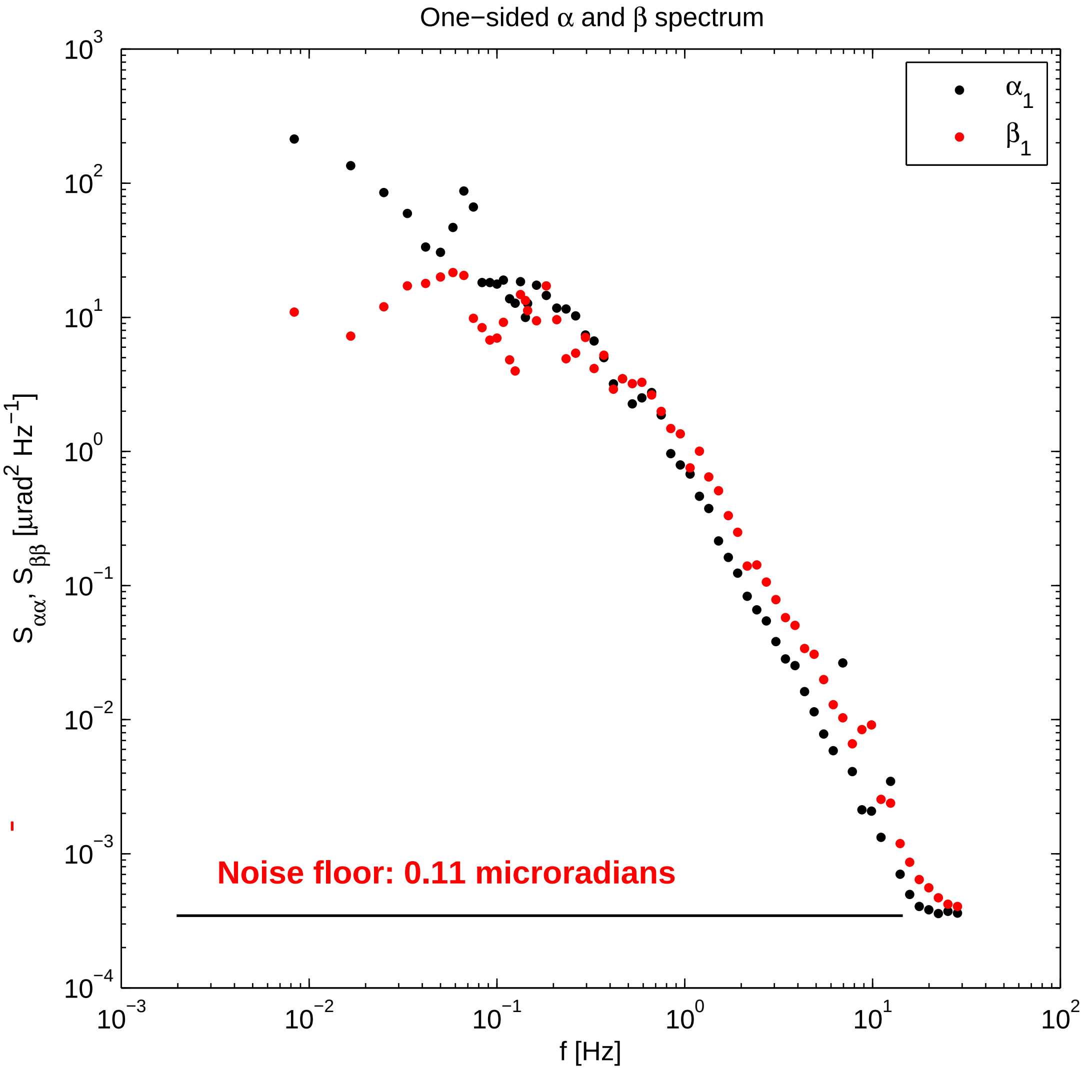

One−sided α and β spectrum
$S_{\alpha\alpha}$, $S_{\beta\beta}$ [μrad^2 Hz^{-1}]
f [Hz]
α_1
β_1
Noise floor: 0.11 microradians
10^{-4}
10^{-3}
10^{-2}
10^{-1}
10^{0}
10^{1}
10^{2}
10^{3}

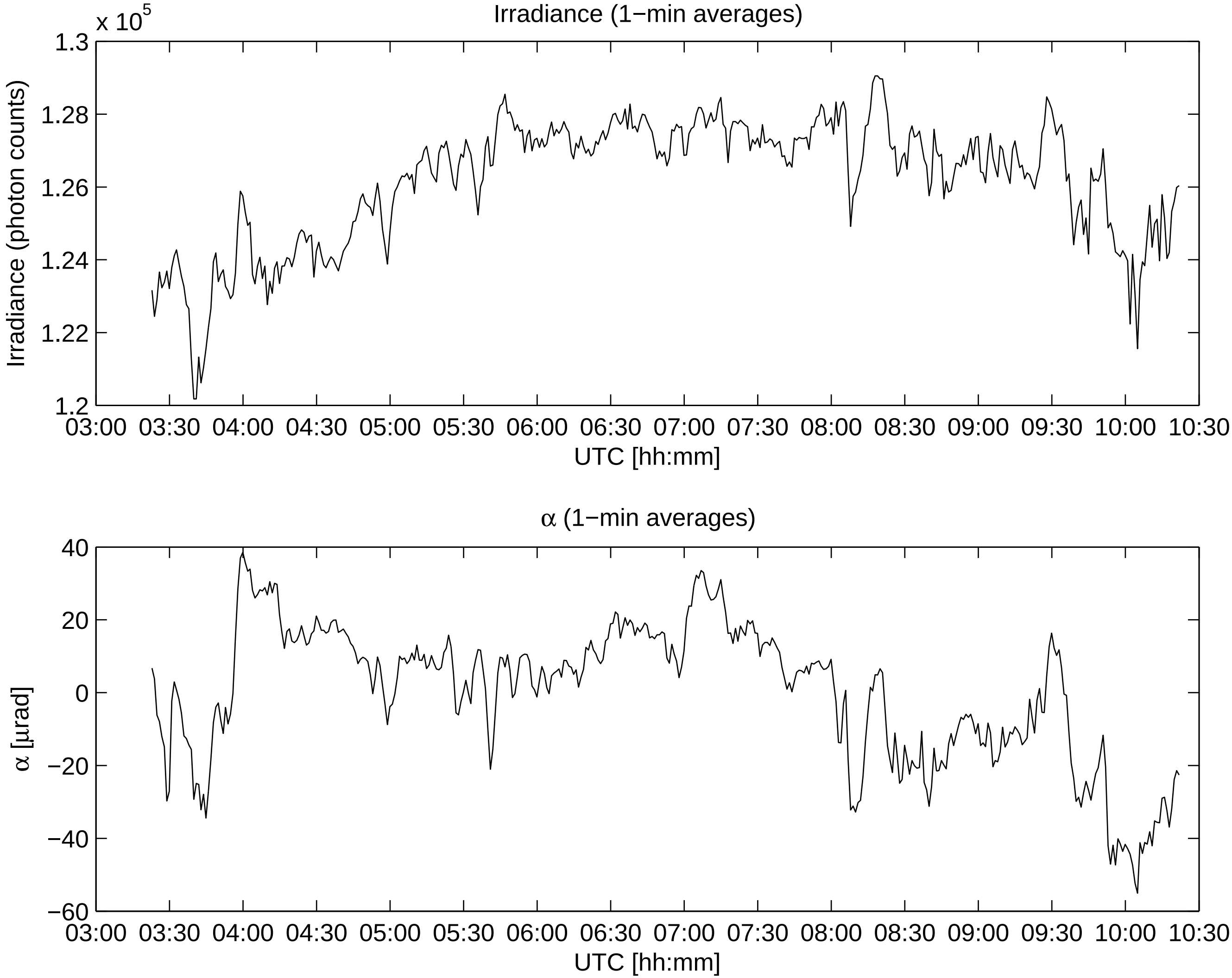

Irradiance (1−min averages)
x 10^5
1.3
1.28
1.26
1.24
1.22
1.2
Irradiance (photon counts)
03:00 03:30 04:00 04:30 05:00 05:30 06:00 06:30 07:00 07:30 08:00 08:30 09:00 09:30 10:00 10:30
UTC [hh:mm]
α (1−min averages)
40
20
0
−20
−40
−60
α [μrad]
03:00 03:30 04:00 04:30 05:00 05:30 06:00 06:30 07:00 07:30 08:00 08:30 09:00 09:30 10:00 10:30
UTC [hh:mm]

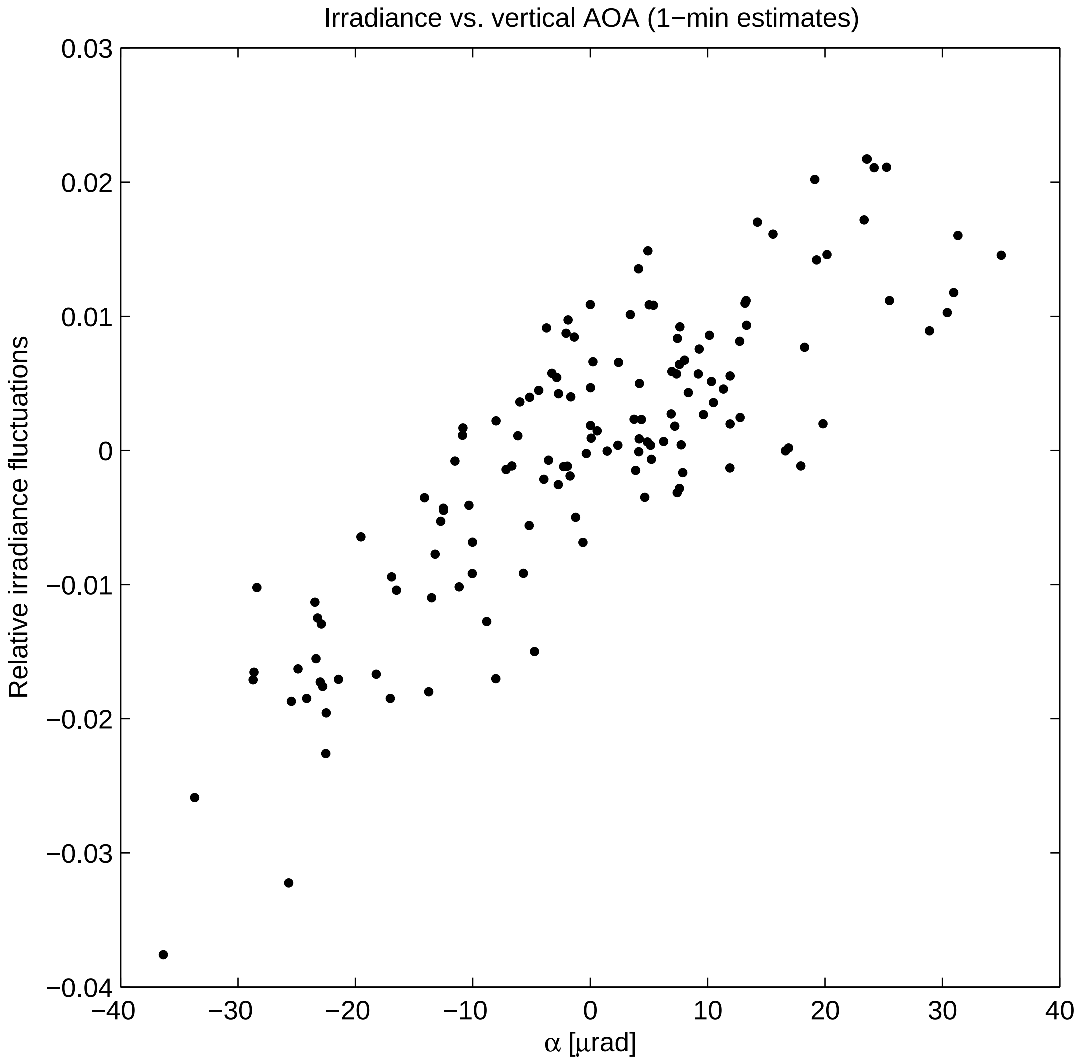
Irradiance vs. vertical AOA (1−min estimates)
0.03
0.02
0.01
0
−0.01
−0.02
−0.03
−0.04
Relative irradiance fluctuations
−40
−30
−20
−10
0
10
20
30
40
α [μrad]

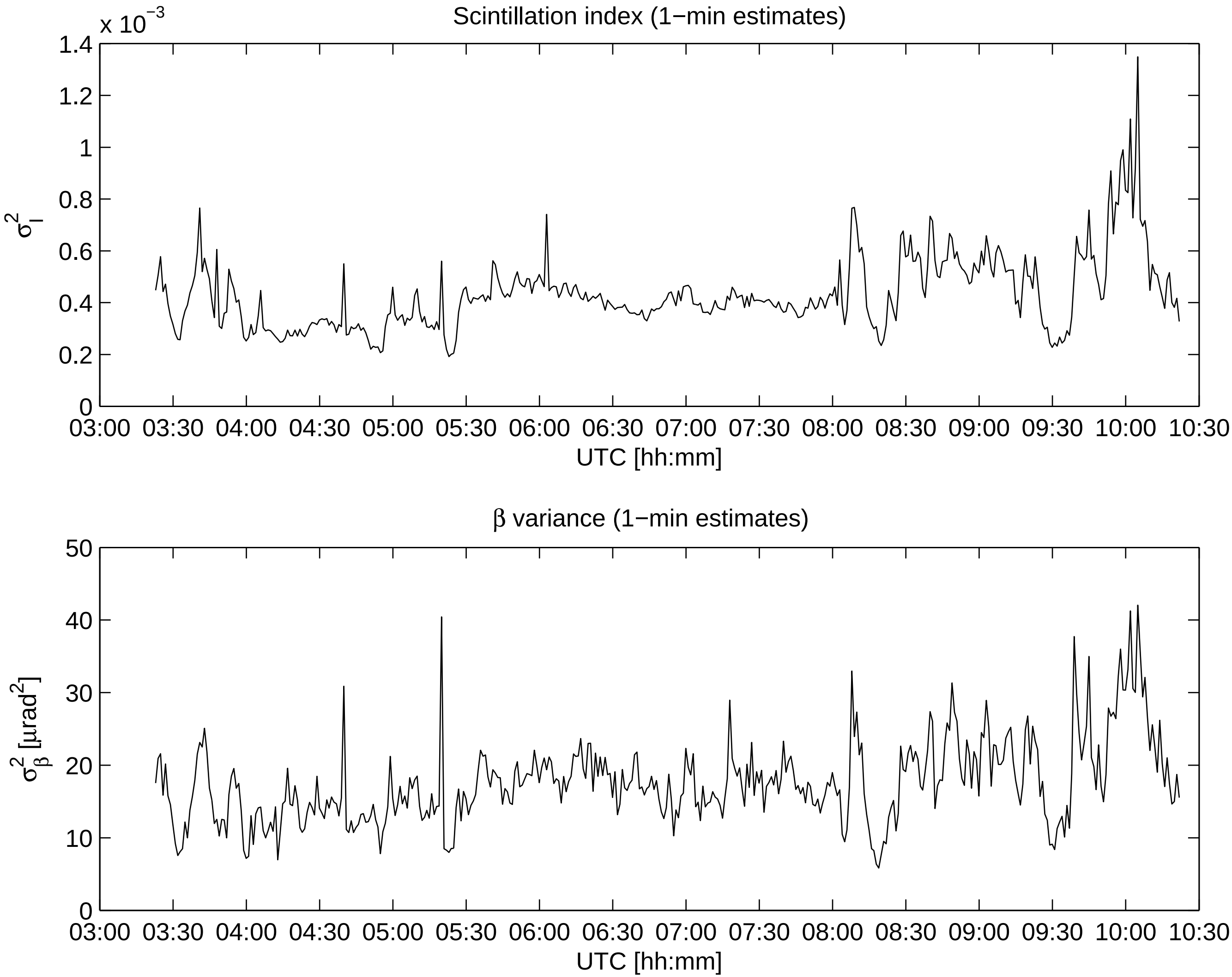

Scintillation index (1−min estimates)
x 10^−3
1.4
1.2
1
0.8
0.6
0.4
0.2
0
σ_I^2
03:00 03:30 04:00 04:30 05:00 05:30 06:00 06:30 07:00 07:30 08:00 08:30 09:00 09:30 10:00 10:30
UTC [hh:mm]
β variance (1−min estimates)
50
40
30
20
10
0
σ_β^2 [μrad^2]
03:00 03:30 04:00 04:30 05:00 05:30 06:00 06:30 07:00 07:30 08:00 08:30 09:00 09:30 10:00 10:30
UTC [hh:mm]

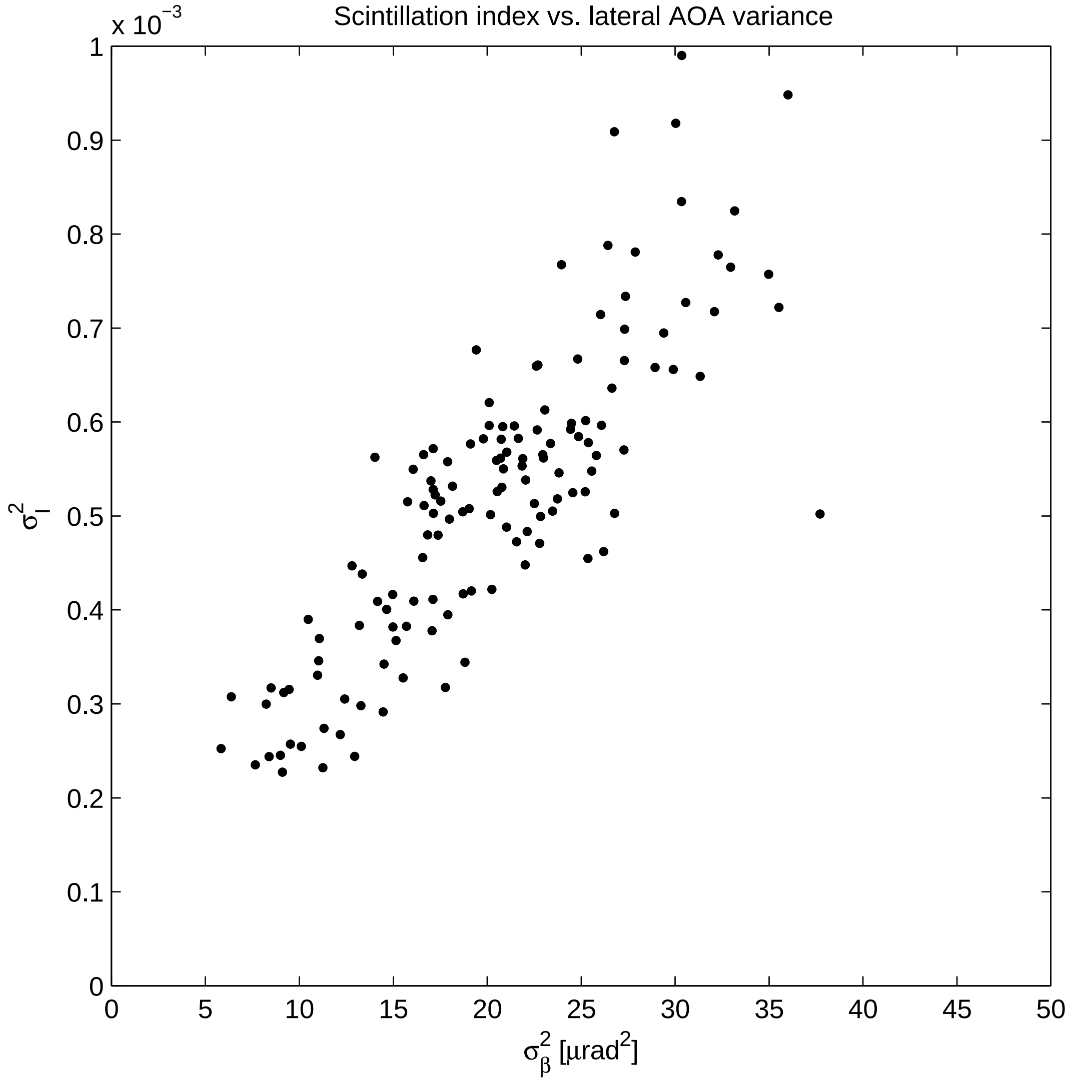
Scintillation index vs. lateral AOA variance
x 10^-3
1
0.9
0.8
0.7
0.6
0.5
0.4
0.3
0.2
0.1
0
σ_I^2
0
5
10
15
20
25
30
35
40
45
50
σ_β^2 [µrad^2]

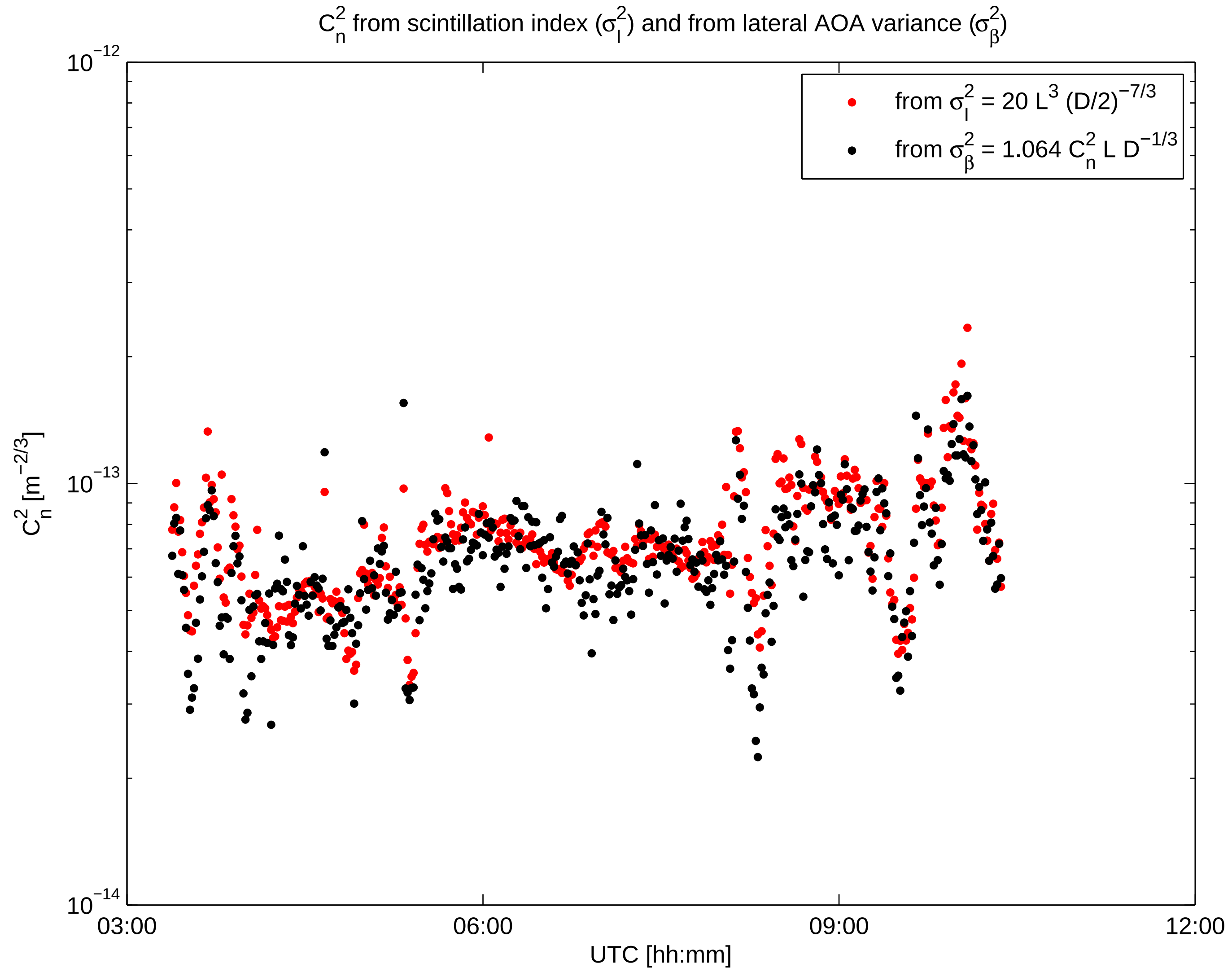

C_n^2 from scintillation index (σ_I^2) and from lateral AOA variance (σ_β^2)
from $\sigma_I^2 = 20\ L^3\ (D/2)^{-7/3}$
from $\sigma_\beta^2 = 1.064\ C_n^2\ L\ D^{-1/3}$
C_n^2 [$m^{-2/3}$]
10^{-12}
10^{-13}
10^{-14}
03:00
06:00
09:00
12:00
UTC [hh:mm]

Retrieval of transverse wind velocities

Basic theory of the AOA spectrum

Assumptions:

- Homogeneous and isotropic inertial-range turbulence in the temperature field
- Taylor's frozen-turbulence hypothesis valid, constant baseline wind speed v_b
- Spherical wave emitted from point source
- Two-point interferometer with baseline length b
- Geometrical optics (frequency f much lower than Fresnel frequency $v_b/\sqrt{L\lambda}$)

Clifford (*J. Opt. Am. Soc. A*, 1971)
and Cheon, Hohreiter, Behn, and Muschinski (*J. Opt. Am. Soc. A*, 2007) predict:

$$S_\beta(f) = \frac{2^{4/3}}{9\pi^{7/6}\Gamma(5/6)} C_n^2 v_b^{5/3} L b^{-2} f^{-8/3} \left[1 - \frac{\sin(2\pi b f/v_b)}{2\pi b f/v_b}\right], \qquad (1)$$

where C_n^2 = refractive-index structure parameter,
L = path length,
f = frequency,
β = horizontal AOA (fluctuation).

Two special cases

High frequencies, $f \gg v_b/b$ (aperture filtering):

$$S_\beta(f) = \frac{2^{4/3}}{9\pi^{7/6}\Gamma(5/6)} C_n^2 v_b^{5/3} L b^{-2} f^{-8/3}. \tag{2}$$

Low frequencies, $f \ll v_b/b$ (no aperture filtering):

$$S_\beta(f) = \frac{2^{7/3}}{27\pi^{1/6}\Gamma(11/6)} C_n^2 v_b^{-1/3} L f^{-2/3}. \tag{3}$$

"Knee frequency" (frequency of intersection of the asymptotes):

$$v_k = \frac{\sqrt{6}}{2\pi}\frac{v_b}{b} = 0.39\frac{v_b}{b}. \tag{4}$$

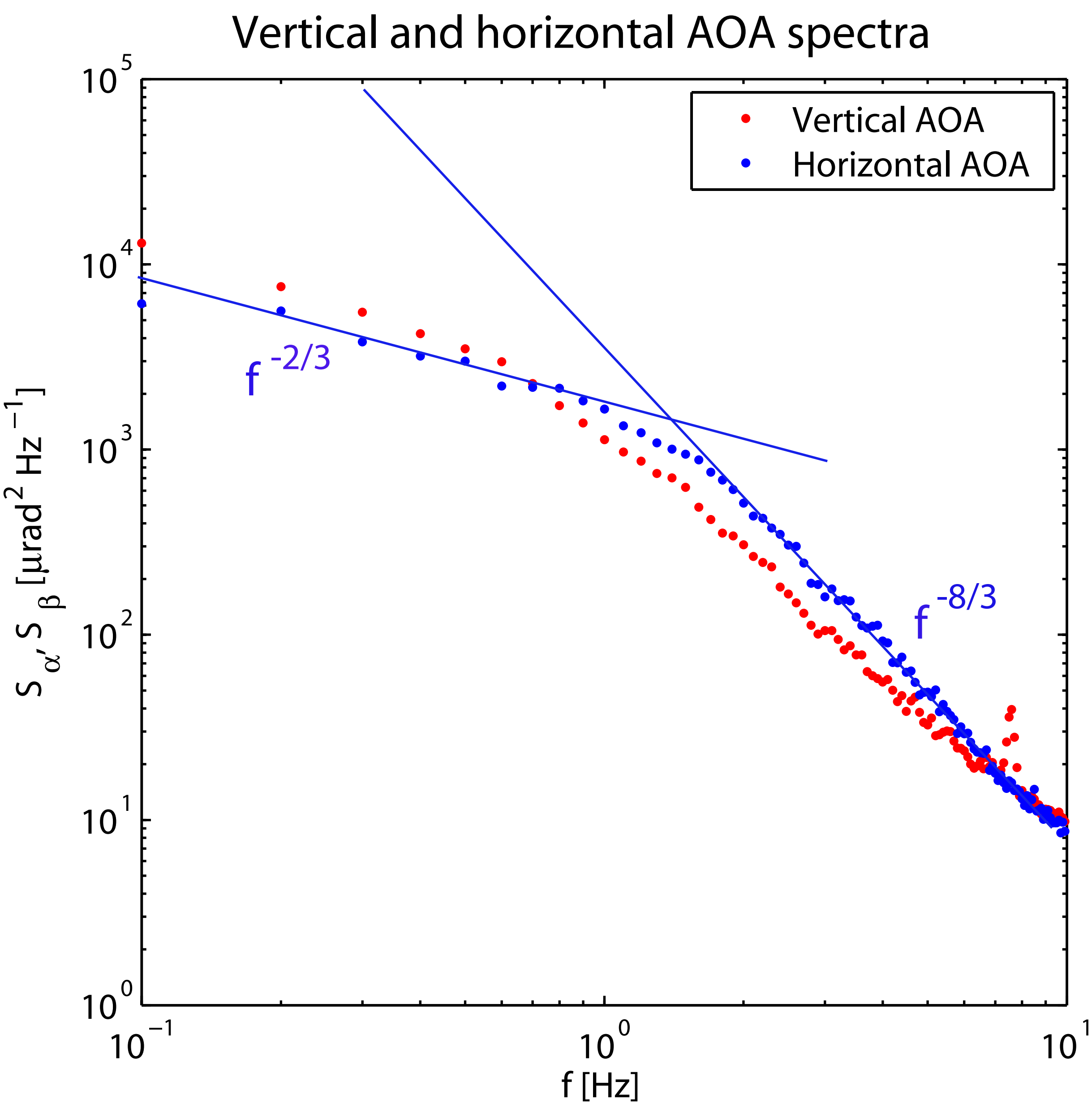

Vertical and horizontal AOA spectra
Vertical AOA
Horizontal AOA
$f^{-2/3}$
$f^{-8/3}$
S_α, S_β [μrad^2 Hz^{-1}]
f [Hz]
10^{-1}
10^0
10^1
10^0
10^1
10^2
10^3
10^4
10^5

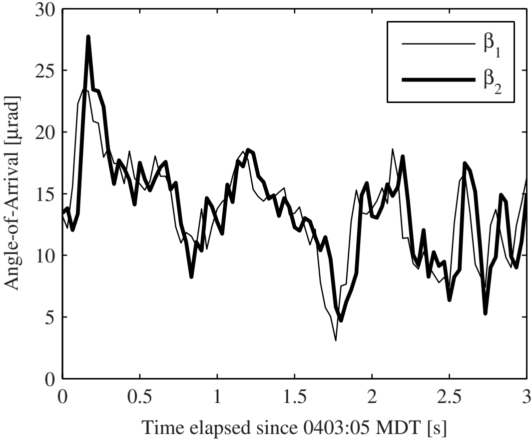

30
25
20
15
10
5
0
Angle-of-Arrival [μrad]
0
0.5
1
1.5
2
2.5
3
Time elapsed since 0403:05 MDT [s]
β1
β2

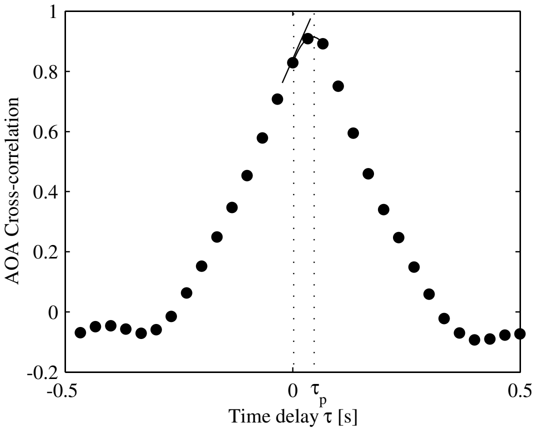

1
0.8
0.6
0.4
0.2
0
-0.2
AOA Cross-correlation
-0.5
0
τ_p
0.5
Time delay τ [s]

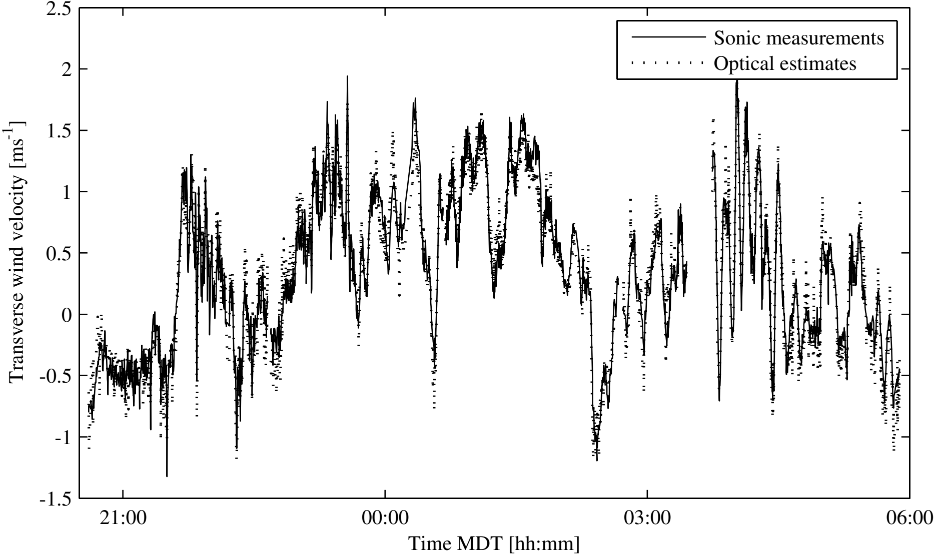
Sonic measurements
Optical estimates
Transverse wind velocity [ms-1]
Time MDT [hh:mm]
2.5
2
1.5
1
0.5
0
-0.5
-1
-1.5
21:00
00:00
03:00
06:00

Summary and conclusions

- Our propagation testbed enables us to quantitatively test hypotheses and approximations about optical propagation through the turbulent atmosphere

- Aperture-averaged AOAs (vertical and lateral) and irradiances contain valuable information about turbulent and non-turbulent characteristics in the atmospheric wind and refractive-index fields.

Future work

- Investigate propagation scenarios involving longer ranges and multiple paths (multiple source/receiver combinations)

- Investigate effects of turbulent fluctuations of aerosol concentrations on long-range AOA and irradiance measurements.